ADVANCED MATERIALS

[1] C. Ziegler, *Handbook of Organic Conductive Molecules and Polymers*, (Ed: H. Nalwa), Vol. 3, Wiley, Chichester **1997**, Ch. 13.
[2] W. Gebauer, M. Sokolowski, E. Umbach, *Chem. Phys.* **1998**, *227*, 33.
[3] F. Kouki, P. Spearman, P. Valet, G. Horowitz, F. Garnier, *J. Chem. Phys.* **2000**, *113*, 385.
[4] M. Muccini, M. Schneider, C. Taliani, M. Sokolowski, E. Umbach, D. Beljonne, J. Cornil, J. L. Bredas, *Phys. Rev. B* **2000**, *62*, 6296.
[5] M. Muccini, E. Lunedei, C. Taliani, D. Beljonne, J. Cornil, J. L. Bredas, *J. Chem. Phys.* **1998**, *109*, 10 513.
[6] P. Petelenz, M. Andrzejak, *Chem. Phys. Lett.* **2001**, *343*, 139.
[7] M. A. Loi, C. Martin, H. R. Chandrasekhar, M. Chandrasekhar, W. Graupner, F. Garnier, A. Mura, G. Bongiovanni, *Phys. Rev. B* **2002**, *66*, 113 102.
[8] W. Gebauer, M. Bassler, R. Fink, M. Sokolowski, E. Umbach, *Chem. Phys. Lett.* **1997**, *266*, 177.
[9] M. Hopmeier, W. Gebauer, M. Oestreich, M. Sokolowski, E. Umbach, R. F. Mahrt, *Chem. Phys. Lett.* **1999**, *314*, 9.
[10] D. Oelkrug, H.-J. Egelhaaf, J. Gierschner, A. Tompert, *Synth. Met.* **1996**, *76*, 249.
[11] F. Meinardi, M. Cerminara, A. Sassella, A. Borghesi, P. Spearman, G. Bongiavanni, A. Mura, R. Tubino, *Phys. Rev. Lett.* **2002**, *89*, 157 403.
[12] F. C. Spano, *J. Chem. Phys.* **2002**, *116*, 5877.
[13] F. C. Spano, *Chem. Phys. Lett.* **2000**, *331*, 7.
[14] F. C. Spano, *J. Chem. Phys.* **2003**, *118*, 981.
[15] Monoclinic, space group $P2_1/c$, see T. Siegrist, C. Kloc, R. A. Laudise, H. E. Katz, R. C. Haddon, *Adv. Mater.* **1998**, *10*, 379.
[16] J. Cornil, D. Beljonne, J.-P. Calbert, J.-L. Brédas, *Adv. Mater.* **2001**, *13*, 1053.
[17] C. Ecoffet, D. Markovitsi, P. Millié, J. P. Lemaistre, *Chem. Phys.* **1993**, *177*, 629.
[18] J. Ridley, M. Zerner, *Theoret. Chim. Acta* **1998**, *32*, 111.
[19] N. Mataga, K. Nishimoto, *Z. Phys. Chem.* **1957**, *13*, 140. The potential between atomic sites A and B is:

$$\gamma_{AB} = \frac{f}{\frac{2f}{\gamma_{AA}+\gamma_{BB}}+r_{AB}} \quad (5)$$

where $f = 1.2$. r_{AB} is the intersite distance, and γ_{AA} and γ_{BB} are the on-site repulsion terms.
[20] D. Beljonne, F. C. Spano, unpublished.
[21] L. B. Clark, M. R. Philpott, *J. Chem. Phys.* **1970**, *53*, 3790.
[22] M. R. Philpott, *Advances in Chemical Physics* (Eds: I. Prigogine, S. A. Rice), Vol. 23, Wiley, New York **1973**.
[23] E. Zojer, N. Koch, P. Puschnig, F. Meghdadi, A. Niko, R. Resel, C. Ambrosch-Draxl, M. Knupfer, J. Fink, J. L. Bredas, G. Liesing, *Phys. Rev. B* **2000**, *61* 16 538.
[24] G. Weiser, S. Moller, *Phys. Rev. B* **2002**, *65*, 45 203.
[25] Note that the herringbone plane for αT6 in Refs. 4 and 5 is the *bc* plane.
[26] S. Moller, G. Weiser, F. Garnier, *Phys. Rev. B* **2000**, *61*, 15 749.
[27] E. A. Silinsh, *Organic Molecular Crystals, Their Electronic States*, Springer, Berlin **1980**.

Single-Crystalline Scroll-Type Nanotube Arrays of Copper Hydroxide Synthesized at Room Temperature**

By *Weixin Zhang*, *Xiaogang Wen*, *Shihe Yang*,* *Yolande Berta*, and *Zhong Lin Wang**

Soon after the discovery of carbon nanotubes,[1] inorganic analogues of the cage structures such as MQ_2 (M = Mo, W; Q = S, Se) were also synthesized.[2] Subsequently, more nested fullerene-like structures of inorganic compounds were fabricated, including BN and V_2O_5.[3] A common feature of the cage-forming materials is their anisotropic 2D layered structures, which tend to bend and eliminate dangling bonds by the intra-layer linkage.

Many methods for the synthesis of inorganic nanotubes have been based on high-temperature processes. These include chemical vapor transport,[4] sol–gel process,[5] arc-discharge,[6] solvothermal treatment,[7] and oxide nanowhisker growth.[8] Low-temperature routes such as templated synthesis have also been attempted,[9,10] but it has proved difficult to form single-crystalline nanotubes.[11] Gedanken et al. have synthesized scroll-like cylindrical GaOOH[12] and nested fullerene-like nanoparticles of Tl_2O and MoS_2 using sonochemical and sonoelectrochemical methods.[13] This soft technique relies on elevated temperatures and pressures at localized spots. Recently, relatively mild conditions of chemical precipitation were adopted for the synthesis of tube-like structures of $Mg(OH)_2$ and NiS.[14]

$Cu(OH)_2$ has a layered structure with inter-layer hydrogen bonds instead of van der Waals interactions occurring in most of the 2D compounds mentioned above. It is tempting to see whether and how nanoscale tubes could be formed from such a layered structure separated by hydrogen bonds. $Cu(OH)_2$ can be conveniently synthesized in solutions of copper(II). Matijević and co-workers have studied the relationship between the morphologies of homogeneously precipitated $Cu(OH)_2$ and the solution compositions.[15,16] The treatment of high-purity copper ribbon in a solution of ammonia and acetone at 277 K for 3 weeks has allowed single crystals of $Cu(OH)_2$ to be grown by Oswald et al.[17] All the crystals were of similar dimensions with tiny hollows or cavities on the surfaces. In this communication, we report the successful growth of a novel scroll-type nanotube structure of $Cu(OH)_2$ arrayed on a copper foil at ambient temperature and pressure. The synthesis was accomplished by surface oxidation of the copper foil in an alkaline aqueous solution with $(NH_4)_2S_2O_8$.

The X-ray diffraction (XRD) pattern of the as-prepared product on copper foil (Fig. 1) is attributable to the orthorhombic $Cu(OH)_2$ phase (space group: $Cmc2_1$) according to the recent refinement of Oswald et al.[17,18] All the diffraction peaks of Figure 1, except those marked with an asterisk, arising from the copper substrate, can be indexed to this phase. The broadening at the leading edge of (111) and the falling edge of (022) indicate the presence of a small amount of CuO due perhaps to dehydration of $Cu(OH)_2$. The calculated cell parameters are: $a_0 = 2.946$ Å, $b_0 = 10.544$ Å, and $c_0 = 5.238$ Å, which are in reasonable agreement with the corresponding literature values: $a_0 = 2.9471$ Å, $b_0 = 10.5930$ Å, and $c_0 = 5.2564$ Å.[17] The intensities of (111), (130), and (020) are significantly enhanced compared to the powder XRD pattern, indicating that the nanotube crystals are on average roughly perpendicular to the copper substrate with a wide distribution of tilts.

The composition inferred from the XRD pattern is consistent with the X-ray photoelectron spectrum (XPS) and the Cu

[*] Prof. S. Yang, Dr. W. Zhang, X. Wen
Department of Chemistry and Institute of Nano Science and Technology
The Hong Kong University of Science and Technology
Clear Water Bay, Kowloon, Hong Kong (China)
E-mail: chsyang@ust.hk
Prof. Z. L. Wang, Y. Berta
School of Materials Science and Engineering
Georgia Institute of Technology
Atlanta, GA 30332-0245 (USA)

[**] This work was supported by an RGC grant administered by the UGC of Hong Kong. We thank MCPF of HKUST for assistance in sample characterization.

  DOI: 10.1002/adma.200304840

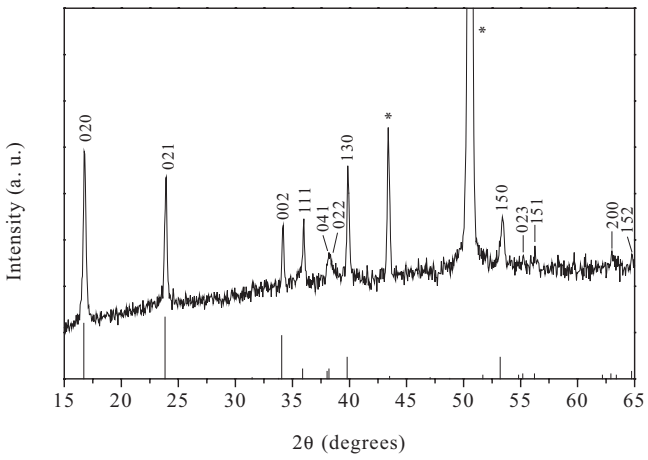

Fig. 1. XRD pattern of the $Cu(OH)_2$ nanotubes grown on a copper foil. The solid lines indicate the XRD pattern of powder $Cu(OH)_2$ (JCPDS Card File 13-0420).

Auger electron spectrum of the as-prepared sample. The Cu 2p XPS spectrum exhibits a peak at 934.9 eV corresponding to Cu $2p_{3/2}$. This, combined with the Cu (L_3MM) Auger electron peak at 570.3 eV, agrees with previous work on bulk $Cu(OH)_2$ and supports the oxidation state of Cu^{2+}.[19,20] The O 1s peak is located at 530.9 eV, which is again consistent with the literature value.[19,20] The atomic ratio of Cu to O is estimated to be 1:1.7, which deviates slightly from the formula of $Cu(OH)_2$ and is partly attributed to the presence of a small amount of CuO. There are no obvious signals from N and S, indicating the absence of ammonia and sulfate in the nanotubes.

Direct observations of the morphologies of the as-prepared samples were made using scanning electron microscopy (SEM) (Fig. 2). The low-magnification SEM image (Fig. 2A) shows that $Cu(OH)_2$ was formed in a wire-like morphology standing upright, and the wires covered a large area of the copper substrate uniformly and compactly. However, the SEM image at a higher magnification (Fig. 2B) reveals the tubular structure of the $Cu(OH)_2$ wires. The nanotubes appear to be roughly circular in cross section, and 50–500 nm in diameter and over 10 μm in length. The contrast at the tube tips shows clear open structures. However, the tip openings are, in general, uneven, irregular, and sometimes present fork-like (arrow a) and polygonal shapes (arrow b). There are also tubes that were formed by curling from the two opposite sides of the sheets until tubular closure (arrow c). In other words, most of the tube tips display apparent scroll-like structures, and the thickness of the tube walls is estimated to be a few tens of nanometers.

Figure 3 shows transmission electron microscopy (TEM) images of the same $Cu(OH)_2$ nanotube sample as used for recording the SEM images in Figure 2. The diameters of the tubes range from 50 to 250 nm, and the lengths of the tubes are shorter due to the sample transfer. Consistent with the SEM observations, the $Cu(OH)_2$ nanotubes all have open tips.

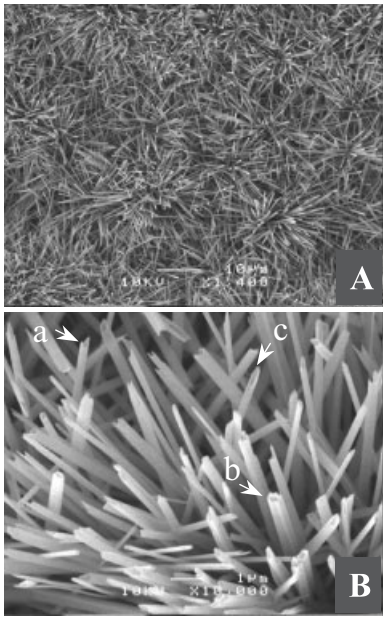

Fig. 2. SEM images of the $Cu(OH)_2$ nanotubes. A) Low magnification (×1400). B) High magnification (×10 000).

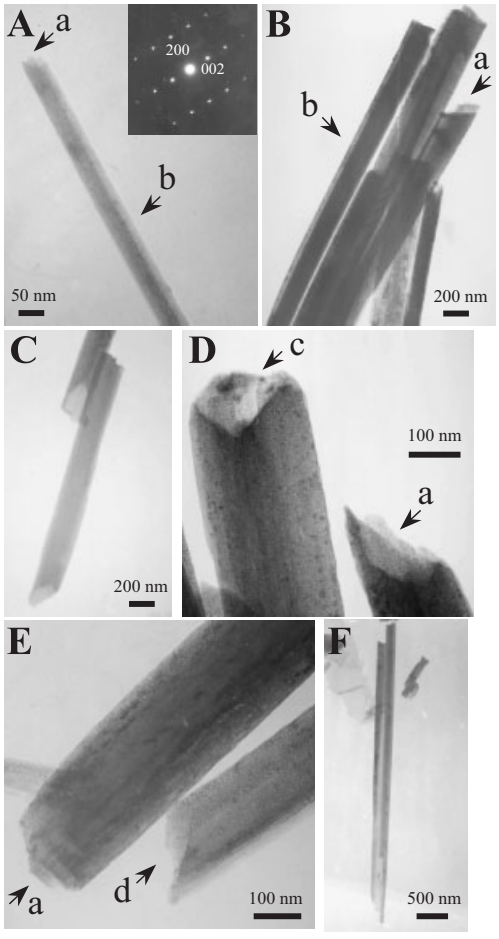

Fig. 3. TEM images of the $Cu(OH)_2$ nanotubes. A) A small nanotube with SAED inset. B) Nanotubes with asymmetric contrast and signatures of the scroll type structure at tip edges. C) Nanotubes with open tips. D) Nanotubes inside nanotubes. E) Nanotubes with an open tip and a protruded scroll at the tip center. F) A dual nanotube rolled from opposite ends.

ADVANCED MATERIALS

Although ordinary tube tips display a single turn (Fig. 3C, arrow d in Fig. 3E), a scrolled tubular structure can be clearly seen for many other tube tips (arrows a in Fig. 3A,B,E). There are at least two or three scrolled layers as seen from the edges. In addition, from some open tips, one can see several smaller tubes wrapped in a big tube (arrow c in Fig. 3D). Asymmetric contrast is perceptible on the tube sides, which indicates the terminals of the scrolls (arrows b in Fig. 3A,B). Such an asymmetric contrast and the scrolled layers mentioned above have also been observed by Gedanken and coworkers for scroll-like nanoparticles of GaOOH.[12] Some twin tubes were formed by rolling from opposite sides of a layer (Fig. 3F). The selected area electron diffraction (SAED) pattern on a 50 nm diameter nanotube (inset of Fig. 3A) demonstrates that the nanotube is single crystalline lying on the (010) plane, with the [100] direction parallel to the longest dimension.

To prove the tubular morphology of the structure, we relied on TEM images. Figure 4A is a bright-field TEM image from a tubular structure, and the corresponding electron diffraction pattern is inset. Due to the single-crystalline structure of the tube, as indicated by the corresponding electron diffraction pattern, the bright-field TEM image shows strong diffraction contrast especially when the electron beam is nearly parallel to a low index zone axis. To minimize the diffraction effect in dark-field TEM imaging, the objective aperture was placed between the diffracted beams to pick up the diffusely scattered electrons, thus the image contrast is expected to be approximately proportional to the thickness-projected mass under the electron beam. The corresponding dark-field TEM image of the tubular structure is given in Figure 4B. Across the tube, the intensity profile shows a flat variation, and the edge surfaces show slightly brighter contrast, suggesting a hollow tubular structure with a very thin shell. Figure 4C is an image recorded when the tube was tilted far off the zone axis to minimize the diffraction effect, which clearly shows the tubular shape.

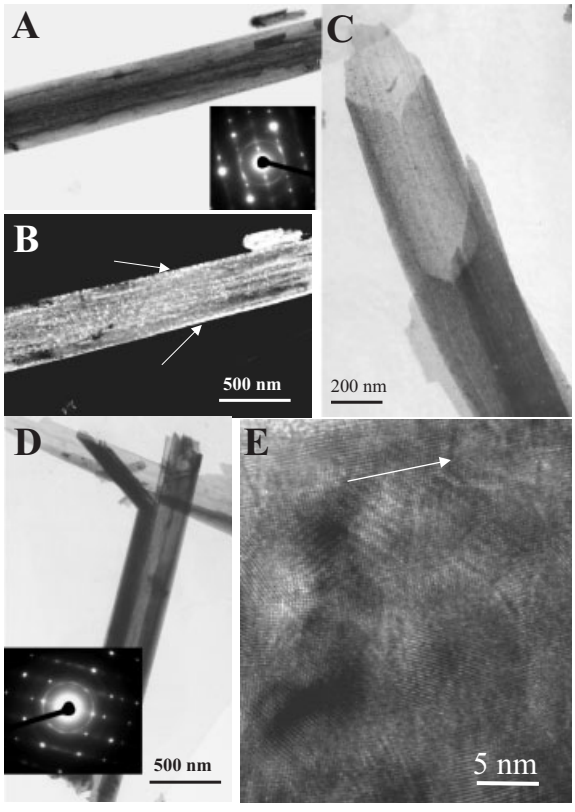

Fig. 4. A) Bright-field and B) corresponding dark-field TEM images of a tubular structure. Inset is the electron diffraction pattern. C) Bright-field TEM of another tubular structure that is oriented at weakly diffracting conditions, so that the tubular shape is apparent. D) TEM of a scroll structure and the corresponding electron diffraction pattern. E) High-resolution TEM image recorded from the wall of a tubular structure. The nanocrystallites are CuO produced by beam radiation damage to the $Cu(OH)_2$.

The tubular entity can be a perfect tube such as the one shown in Figure 4A, or a scroll structure. Figure 4D shows the case where the scroll is not quite closed, thus the overlap of the bent over edges with the backsides can be clearly identified by the thickness-projected mass contrast. Electron diffraction indicates that the structure is single crystalline, which means that the back side and the front side have the same crystal orientation.

The $Cu(OH)_2$ nanotubes are very sensitive to electron beam illumination, and the structure is rapidly damaged due to a transformation from $Cu(OH)_2$ to nanocrystallites of CuO. The rings observed in the diffraction pattern are from CuO nanocrystals. The high-resolution TEM image recorded from the shell of the tube is dominated by CuO, as displayed in Figure 4E. Many nanocrystals ~7–10 nm in size are observed and their orientations are random. It must be pointed out again that this is the result of electron beam radiation damage. The as-synthesized tube is single crystalline.

The reaction that accounts for the $Cu(OH)_2$ nanotube growth is essentially an oxidation process.

$$Cu + 4NaOH + (NH_4)_2S_2O_8 \longrightarrow Cu(OH)_2 + 2Na_2SO_4 + 2NH_3\uparrow + 2H_2O$$

When a copper foil was dipped into the alkaline oxidant solution, a blue solid film of $Cu(OH)_2$ gradually grew on the surface of the copper foil. This reaction was accompanied by the evolution of gas bubbles with an ammoniac pungent odor, indicating the formation of NH_3. Control experiments in less basic solutions (pH 8.0–10.0) under otherwise the same conditions did not produce $Cu(OH)_2$ nanotubes. In this case, only $Cu_4(SO_4)(OH)_6$ was formed as crystalline spindle-shaped sheets. It is only when $[OH^-] > 1$ M that $Cu(OH)_2$ nanotubes could be formed.

The exact mechanism for the formation of the tubular nanostructure is still under investigation. However, they appear to be produced in a complex and highly non-equilibrium reaction system, in which different growth speeds of the crystal faces determine the ultimate morphology.[21] The orthorhombic $Cu(OH)_2$ consists of (olated) chains in the planes (001), which are oriented along [100] and characterized by the square planar coordination of the Cu^{2+} ions with strong $\sigma_{x^2-y^2}$

bonds. The Cu^{2+} ions form another two longer and more ionic bonds with two OH^- groups from neighboring chains along the *c*-axis, completing a deformed octahedron in the first coordination sphere of Cu^{2+}. By juxtaposing the chains in this way, one obtains a corrugated sheet parallel to (010). Essentially, the sheet is formed by edge sharing of the distorted $Cu(OH)_6$ octahedra. A three-dimensional $Cu(OH)_2$ crystal is formed by stacking of the sheets through hydrogen bonds. According to the Bravais–Friedel–Donnay–Harker analysis, the growth speed of such a crystal is normally proportional to $1/d_{hkl}$.[21] The interplanar distance of (010) is the longest (10.60 Å) with relatively loose hydrogen bond linkages. On the other hand, the interplanar distance of (100) is the shortest (2.952 Å), and therefore the nanotubes grow along the [100] direction by scrolling the sheet parallel to (010).

In alkaline aqueous solution, the surfaces of the copper foils were rapidly oxidized to Cu^{2+} by the oxidant $(NH_4)_2S_2O_8$ after 2–3 min. Then the highly alkaline conditions favored the square planar coordination of OH^- groups to Cu^{2+}, giving rise to stoichiometric chains along [100]. These chains were then connected along the *z*-axis through the bridging OH^- groups. The resulting two-dimensional layers parallel to (010) are connected through H bonds in an asymmetric fashion with respect to the layers. Conceivably, under highly basic conditions, the inter-layer H-bond linkage at the sheet edges may be weakened. This, together with the asymmetric layer structure, caused stresses in the layers. Consequently, the nanosheets rolled so as to relieve the stresses, forming the final tubular structure. The adsorption of NH_3 seems to be relatively unimportant because the use of the oxidant $Na_2S_2O_8$ instead of $(NH_4)_2S_2O_8$ for the synthesis of $Cu(OH)_2$ nanotubes gave similar results.

In summary, a novel layer-rolled tubular nanostructure of $Cu(OH)_2$ has been synthesized on a copper foil by a simple liquid–solid reaction under alkaline and oxidative conditions. The $Cu(OH)_2$ nanotubes were 50–500 nm in diameter and over 10 μm in length, and they could be grown as free-standing arrays on copper substrates. The advantages of our method for the preparation of inorganic nanotubes lie in its simplicity, high yield, mild reaction conditions, and the ability to produce nanotubes as single crystals and in the form of arrays. Therefore, it offers an attractive and convenient path to large-scale synthesis of phase pure inorganic nanotube arrays.

Experimental

Stock solutions of sodium hydroxide (10.0 mol dm^{-3}) and ammonium persulfate (1 mol dm^{-3}) were prepared by dissolving NaOH (99–100.5 %, Riedel–de Haën) and $(NH_4)_2S_2O_8$ (98 %, Riedel–de Haën) in deionized water, respectively, and stored in glass bottles. High-purity copper foils (99.99 %, Aldrich) were used as received. A typical synthesis was performed as follows. A yellow solution was prepared in a 20 mL glass bottle by mixing 4 mL of the NaOH solution, 2 mL of the $(NH_4)_2S_2O_8$ solution, and 9 mL of deionized water. A piece of clean copper foil (10.00 mm × 3.00 mm × 0.25 mm) was immersed into the solution. A few minutes later, a faint blue color appeared on the copper foil surface, and the initial yellow solution became increasingly blue. In 15 min, a light blue film covered the copper foil surface. When the color of the film became deep blue, the copper foil was taken out from the solution, rinsed with deionized water and absolute ethanol, and dried in air.

X-ray diffraction (XRD) analysis was performed on a Philips PW 1830 X-ray diffractometer with a 1.5405 Å Cu Kα rotating anode point source. The source was operated at 40 kV and 40 mA, and the Kβ radiation was eliminated using a nickel filter. Transmission electron microscopy (TEM) measurements were conducted with Philips CM20, JEOL 2010, and Hitachi HF-2000 transmission electron microscopes, using an accelerating voltage of 200 kV. The $Cu(OH)_2$ nanotubes on copper foils were transferred to carbon films on copper grids by allowing them to touch and then slide gently relative to each other. The morphologies were examined on a JEOL JSM-6300F scanning electron microscope (SEM) at an accelerating voltage of 10 kV. To prevent charging, a thin film of gold was sputtered on the sample surface. For X-ray photoelectron spectroscopy (XPS), a Physical Electronics PHI 5600 multi-technique system was used with a monochromatic Al Kα X-ray source.

Received: December 21, 2002

[1] S. Iijima, *Nature* **1991**, *354*, 56.
[2] a) R. Tenne, L. Margulis, M. Genut, G. Hodes, *Nature* **1992**, *360*, 444. b) Y. Feldman, E. Wasserman, D. J. Srolovitz, R. Tenne, *Science* **1995**, *267*, 222.
[3] a) W. Tremel, *Angew. Chem. Int. Ed*. **1999**, *38*, 2175. b) G. R. Patzke, F. Krumeich, R. Nesper, *Angew. Chem. Int. Ed*. **2002**, *41*, 2446. c) R. Tenne, A. K. Zettl, *Top. Appl. Phys.* **2001**, *80*, 81.
[4] a) M. Remskar, Z. Skraba, M. Regula, C. Ballif, R. Sanjinés, F. Lévy, *Adv. Mater*. **1998**, *10*, 246. b) M. Nath, C. N. R. Rao, *J. Am. Chem. Soc*. **2001**, *123*, 4841.
[5] a) L. Margulis, G. Salitra, R. Tenne, M. Talianker, *Nature* **1993**, *365*, 113. b) H. Nakamura, Y. Matsui, *J. Am. Chem. Soc*. **1995**, *117*, 2651. b) M. E. Spahr, P. Bitterli, R. Nesper, M. Muller, F. Krumeich, H.-U. Nissen, *Angew. Chem. Int. Ed*. **1998**, *37*, 1263.
[6] A. Loiseau, F. Willaime, N. Demoncy, G. Hug, H. Pascard, *Phys. Rev. Lett*. **1996**, *76*, 4737.
[7] a) Y. Jiang, Y. Wu, S. Zhang, C. Xu, W. Yu, Y. Xie, Y. T. Qian, *J. Am. Chem. Soc*. **2000**, *122*, 12 383. b) X. Zheng, Y. Xie, L. Zhu, X. Jiang, Y. Jia, W. Song, Y. Sun, *Inorg. Chem*. **2002**, *41*, 455.
[8] a) A. Rothschild, G. L. Frey, M. Homyonfer, M. Rappaport, R. Tenne, *Mater. Res. Innov*. **1999**, *3*, 145. b) A. Rothschild, J. Sloan, R. Tenne, *J. Am. Chem. Soc*. **2000**, *122*, 5169.
[9] a) C. M. Zelenski, P. K. Dorhout, *J. Am. Chem. Soc*. **1998**, *120*, 734. b) C. R. Martin, *Acc. Chem. Res.* **1995**, *28*, 61.
[10] a) P. M. Ajayan, O. Stephan, P. Redlich, C. Colliex, *Nature* **1995**, *375*, 564. b) C. N. R. Rao, B. C. Satishkumar, A. Govindaraj, *Chem. Commun*. **1997**, 1581.
[11] a) T. Kasagu, M. Hiramatsu, A. Hoson, T. Sekino, K. Niihara, *Langmuir* **1998**, *14*, 3160. b) T. Kasagu, M. Hiramatsu, A. Hoson, T. Sekino, K. Niihara, *Adv. Mater*. **1999**, *11*, 1307. c) S. M. Liu, L. M. Gan, L. H. Liu, W. D. Zhang, H. C. Zeng, *Chem. Mater*. **2002**, *14*, 1391.
[12] S. Avivi, Y. Mastai, G. Hodes, A. Gedanken, *J. Am. Chem. Soc*. **1999**, *121*, 4196.
[13] a) Y. Mastai, M. Homyonfer, A. Gedanken, G. Hodes, *Adv. Mater*. **1999**, *11*, 1010. b) S. Avivi, Y. Mastai, A. Gedanken, *J. Am. Chem. Soc*. **2000**, *122*, 4331.
[14] a) Y. Li, M. Sui, Y. Ding, G. Zhang, J. Zhuang, C. Wang, *Adv. Mater*. **2000**, *12*, 818. b) X. Jiang, Y. Xie, J. Lu, L. Zhu, W. He, Y. T. Qian, *Adv. Mater*. **2001**, *13*, 1278.
[15] a) S. Kratohvil, E. Matijevic, *J. Mater. Res.* **1991**, *6*, 766. b) S. H. Lee, Y. S. Her, E. Matijevic, *J. Colloid Interface Sci*. **1997**, *186*, 193.
[16] R. Rodríguez-Clemente, C. J. Serna, M. Ocaña, E. Matijevic, *J. Cryst. Growth* **1994**, *143*, 277.
[17] H. R. Oswald, A. Reller, H. W. Schmalle, E. Dubler, *Acta Crystallogr*. **1990**, *C46*, 2279.
[18] H. Jaggi, H. R. Oswald, *Acta Crystallogr*. **1961**, *14*, 1041.
[19] C. D. Wagner, W. M. Riggs, L. E. Davis, J. F. Moulder, in *Handbook of X-ray Photoelectron Spectroscopy* (Ed: G. E. Muilenberg), Perkin-Elmer Corp., Eden Praire, MN **1979**.
[20] a) K. L. Chavez, D. W. Hess, *J. Electrochem. Soc*. **2001**, *148*, G640. b) J. Hernandez, P. Wrschka, G. S. Oehrlein, *J. Electrochem. Soc*. **2001**, *148*, G389.
[21] a) P. Hartman, in *Crystal Growth: An Introduction* (Ed: P. Hartman), North-Holland, Amsterdam **1973**, p. 3. b) P. Hartman, W. G. Perdok, *Acta Crystallogr*. **1955**, *8*, 49. c) A. W. Vere, in *Crystal Growth: Principles and Progress* (Ed: P. J. Dobson), Plenum Press, New York **1987**, p. 17. d) X. G. Wen, W. X. Zhang, S. H. Yang, Z. R. Dai, Z. L. Wang, *Nano Lett.* **2002**, *2*, 1397.

